

OPEN Humid heat waves at different warming levels

Simone Russo^{1,2}, Jana Sillmann³ & Andreas Sterl 60⁴

Received: 5 April 2017 Accepted: 7 July 2017

Published online: 07 August 2017

The co-occurrence of consecutive hot and humid days during a heat wave can strongly affect human health. Here, we quantify humid heat wave hazard in the recent past and at different levels of global warming. We find that the magnitude and apparent temperature peak of heat waves, such as the ones observed in Chicago in 1995 and China in 2003, have been strongly amplified by humidity. Climate model projections suggest that the percentage of area where heat wave magnitude and peak are amplified by humidity increases with increasing warming levels. Considering the effect of humidity at 1.5° and 2° global warming, highly populated regions, such as the Eastern US and China, could experience heat waves with magnitude greater than the one in Russia in 2010 (the most severe of the present era). The apparent temperature peak during such humid-heat waves can be greater than 55 °C. According to the US Weather Service, at this temperature humans are very likely to suffer from heat strokes. Humid-heat waves with these conditions were never exceeded in the present climate, but are expected to occur every other year at 4° global warming. This calls for respective adaptation measures in some key regions of the world along with international climate change mitigation efforts.

High temperatures and heat waves are known for their impacts on human health, for instance reflected in higher mortality rates¹. The impact of heat waves can be due to a single variable, such as extreme temperature, or to a combination of variables not all of which are necessarily extreme². In humid regions, the estimation of heat wave magnitude based only on temperature may underestimate the severity of a heat wave, as high humidity during consecutive hot days can be a contributory factor to amplify the effect of extreme heat waves^{3–5}. In climatology, the occurrence of at least three consecutive hot days has been defined as a heat wave⁶⁻⁹. Here a heat wave is considered humid if at least one of its days shows an Apparent Temperature¹⁰ (hereafter AT, often referred to as heat index) that exceeds the dry-bulb temperature (T, in this case daily maximum temperature, see method). The AT is used to take into account the effect of relative humidity during hot days. It represents a non-linear measure of temperature and relative humidity¹¹, which are generally negatively correlated^{12, 13}, (Supplementary Fig. S1). For physiological stress, relative humidity is relevant because it describes the ability to lose heat through evaporative cooling^{11,}

To take into account the effect of relative humidity during consecutive hot days, we introduce the new Apparent Heat Wave Index (AHWI), which is calculated analogously to the Heat Wave Magnitude Index daily HWMId¹⁵, but with daily maximum temperature replaced by AT for those heat wave days with AT > T (see method). We use two reanalysis sets (ERA-Interim¹⁶ and NCEP-2¹⁷) to compare the new AHWI, calculated with daily maximum temperature and daily minimum relative humidity (see method), with the existing HWMId¹⁵, which is based on temperature only.

Additionally, by using daily maximum temperature and minimum relative humidity outputs from the Coupled Model intercomparison Project Phase 5 (CMIP5¹⁸), we project heat wave and apparent heat wave magnitudes at different warming levels (1.5°, 2° and 4°) relative to the period 1861–1880 (see method). In order to show the potential impact of the combination of temperature and relative humidity on human health during a heat wave, we consider AT peak (AT_{peak}) defined as the maximum AT value during a heat wave (see method).

We analyze changes in the yearly probability of AT_{peak} higher than 40 °C (~105°F, hereafter AT40C) and 55 °C (~130° F, hereafter AT55C). These thresholds are the ones at which the US National Weather Service issues a heat advisory because of dangerous health conditions (high incidence of heat cramps, heat exhaustion and heat strokes) and very dangerous health conditions (heat stroke very likely), respectively.

¹European Commission, Joint Research Centre, Ispra, Italy. ²Institute for Environmental Protection and Research (ISPRA), Rome, Italy. ³Center for International Climate and Environmental Research (CICERO), Pb. 1129 Blindern, N-0318, Oslo, Norway. ⁴Royal Netherlands Meteorological Institute (KNMI), De Bilt, Netherlands. Correspondence and requests for materials should be addressed to S.R. (email: simone.russo@ec.europa.eu)

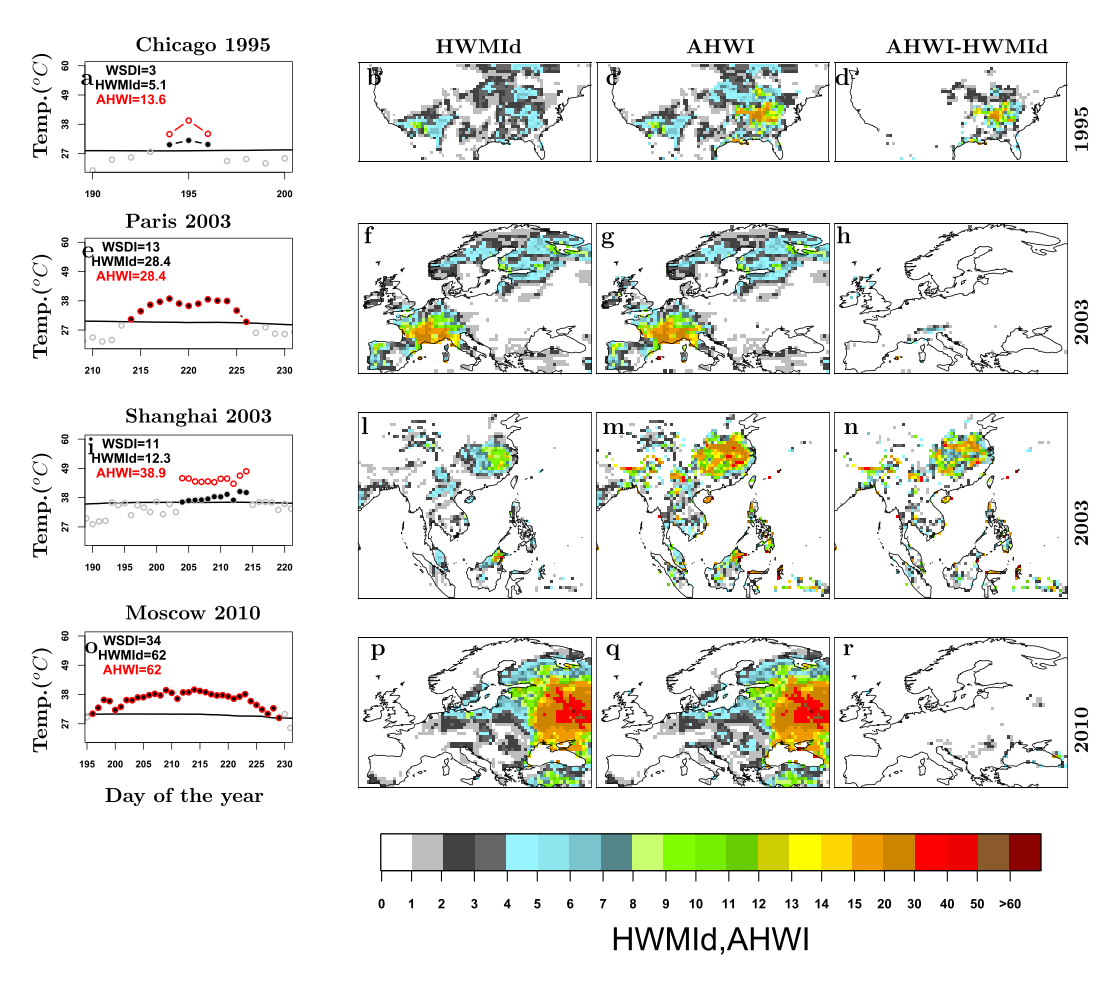


Figure 1. Historical heat waves and humid heat waves across world regions with different climates and their HWMId and AHWI spatial distribution. The panels (**a**,**e**,**i**,**o**) show time series of heat waves that occurred in specific locations reporting the values of HWMId, AHWI and the duration, calculated by means of the Warm Spell Duration Index (WSDI, see method). Black line is the 90th percentile daily threshold (see method). Open grey circles are the temperature values of the days. Full black circles are the days in the heat wave. Red open circles represent the apparent temperature values calculated, for each day composing the heat wave, by means of the Heat Index (see method). The maps in (**b**,**f**,**l**,**p**) and (**c**,**g**,**m**,**q**) represent the spatial distribution of the HWMId and AHWI, respectively. The maps in (**d**,**h**,**n**,**r**) show the spatial distribution of the differences between AHWI and HWMId. This figure has been produced using R version 3.3.2 (https://cran.r-project.org/).

Results

The spatial distribution of the 90th percentile of the HWMId and AHWI calculated at each grid point within the period 1979–2015 compares well between reanalysis (ERA-Interim and NCEP-2) and model data (see Supplementary Figs S2 and S3). Additionally, the HWMId, AHWI, and AT40C spatial patterns compare remarkably well across models (Supplementary Figs S4, S5 and S6, respectively) and strongly resemble the reanalysis (Supplementary Figs. S2a,b,d,e and S3a,b) and ensemble models patterns (Supplementary Figs S2c,f and S3c). These results confirm those of a recent study¹⁹ showing robust agreement in heat stress variables (based on temperature and relative humidity) in a set of CMIP5 models.

In some key regions, such as the Midwestern and Eastern US, China, Northern Latin America and Malaysia, both reanalysis and model data show that heat wave magnitude and peak temperature have been amplified by high relative humidity in the recent past. The selected heat waves of Chicago 1995 and Shanghai 2003 are clear examples of the contribution of relative humidity during a heat wave (Fig. 1a-d,i-n). On the contrary, the effect of relative humidity was negligible during the two famous heat waves that occurred in Central Europe in 2003 and in Russia in 2010 (Fig. 1e-h,o-r).

In both humid and dry regions heat wave occurrence can be associated with persistent synoptic conditions such as: blocking patterns, reduced cloudiness and advection of warm air^{20, 21}. However, in regions such as the Eastern US and China, where apparent temperature impacts are amplified by high relative humidity, the formation of a humid heat wave typically is due to hot and humid air being advected from the Gulf of Mexico or from tropical regions²², respectively. In contrast, across Europe and the Western US, the formation of a dry heat wave is

often due to a blocking pattern and associated advection of hot dry air from desert areas. As an example the 2010 Russian heat wave resulted from a strong blocking anticyclone driving warm air from Africa²³.

During the heat wave of 1995, Chicago was referred to as "the Urban Inferno²⁴". The heat wave had a high impact because extreme temperatures were made worse by high relative humidity, which made it difficult to sweat and cool off. From a physiological point of view, this short heat wave would not have been so extreme without high relative humidity^{25, 26} (Fig. 1a–d).

In the summer of 2003, two heat waves hit Europe²¹ and China²⁷ (Fig. 1e-h,i-n, respectively). By comparing these two events, we see that the heat wave across central Europe was mainly due to extreme temperatures, whereas during the hottest summer of the past 50 years recorded in Shanghai in 2003 high relative humidity played an important role in exacerbating the heat wave impact²⁷ (Fig. 1i-n).

Another example of extreme but not humid heat wave is represented by the heat wave that occurred in Russia in the summer of the 2010 (Fig. 1o-r). This heat wave is considered the most extreme one of the present era^{15, 21}. For this heat wave the maximum magnitude exceeded the score of 60 (Fig. 1o-r), a value that, according to all our datasets, was never recorded during any other heat wave of the recent past period (1979–2015). Additionally, the HWMId and AHWI values calculated for the same recent past period from the CMIP5 models do not show any location exceeding a magnitude of 60. This threshold is used as reference to estimate the probability of occurrence of an extreme heat wave with magnitude greater than the one in Russia in 2010 (hereafter, RU2010).

In the coming decades, with increasing global mean temperature, the global land fraction with high probability of occurrence of humid heat waves with magnitude greater than RU2010 is expected to increase (Fig. 2). On a global scale, the near-surface *absolute humidity* of the air roughly follows the increasing temperatures according to the Clausius–Clapeyron relationship, and thus *relative humidity* remains roughly constant or slightly decreases over land²⁸. However, locally the relative humidity may change due to circulation changes²⁸. Moreover, the non-linear terms in the definition of AT amplify the impact of temperature changes even if relative humidity remains constant. The humidity-induced heat stress amplification is strongest in the regions that are warmest and most humid under present-day conditions^{19, 29} Our results are consistent with earlier studies showing that heat stress is projected to increase over all land regions along with rising temperatures¹⁹.

At 1.5 °C and 2 °C warming above pre-industrial levels, the probability of occurrence of a RU2010 heat wave is zero almost everywhere if measured with the HWMId (Fig. 2b,c). On the contrary, this probability is different than zero, although still very small, in the Eastern US, China, Central West Africa and Northern Latin America when measured by means of the AHWI, which takes into account both temperature and relative humidity (Fig. 2e,f). At 4 °C warming the yearly probability of occurrence of a heat wave with magnitude greater than the RU2010 will be greater than 10% in Central Europe, India, and across many African regions. The Eastern US, Northern Latin America and China are expected to experience such type of heat waves with a annual probability greater than 50%, corresponding to an average return period of two years (Fig. 2g). This probability is greater than the one projected in the hottest world regions, such as the Arabian Peninsula, Australia and other dry-deserts (see Fig. 2d,g).

Similar results are found for the occurrence of heat waves with AT40C and AT55C peaks. The percentage of global land area with a high probability of occurrence of heat waves with AT40C and AT55C increases with increasing warming levels (Fig. 3). Across the hottest world regions and the regions where relative humidity amplifies the heat wave magnitude, the probability of annual occurrence of a heat wave with a AT40C peak show annual values exceeding 50% and 90% at a warming level of 2 °C and 4 °C, respectively (Fig. 3b,c). These probability values are much smaller if measured only with temperature (see supplementary Fig. S7a–c). Highly populated regions, such as the Eastern US and China, are expected to experience the warmest AT_{peak} values of the world (see Supplementary Fig. S8), with an occurrence of a AT55C peak on a two year basis (probability greater than 50%, see Fig. 3f). Due to the high expected apparent temperature values these regions are projected to have high number of deaths among people older than 65 years in 2050³⁰, without assuming adaptation effects. Note that, as for the heat wave magnitude across these regions, all warming levels show a probability of occurrence of AT55C equal to or greater than the one of the warmest world regions such as dry-deserts (Fig. 3d–f). Without considering relative humidity, the probability that heat wave temperature peaks exceed 55 °C is equal or very close to zero almost everywhere at all warming levels (see Fig. S7d–f).

The occurrence of heat waves with AT55C, never recorded in our data records in the recent past, is likely to cause heat strokes by limiting the human thermoregulation. The exceedance of this apparent temperature across these regions is in agreement with other measures accounting for the combined effect of temperature and relative humidity. As an example, the wet-bulb temperature peak during a heat wave is expected to exceed the value of 35 °C (see Supplementary Fig. S9), a threshold likely to induce hyperthermia in humans and other mammals as dissipation of metabolic heat becomes impossible^{25, 31} While this never happens in the present climate, and it is unlikely at 1.5 °C and 2 °C, it would occur on a regular basis in many highly populated regions with global-mean warming of about 4 °C, questioning the habitability of some of these regions.

Discussion

Our results show that some of the most densely populated regions are among those that are most exposed to humid heat waves. In the recent past, the severity of heat waves across urban areas, such as Chicago and Shanghai, that are considered non-severe from a temperature-only point of view, was strongly increased when considering relative humidity. Due to the humidity effect the AT_{peak} values across these cities are projected to reach extremely severe values in the future with the rising of global mean temperature. At 4 °C global warming, the apparent heat wave magnitude is greater than the highest present value, with AT_{peak} exceeding the level of 55 °C, (critical for human survival) at least once in two years. The effect of relative humidity on the heat wave magnitude and peak might even be underestimated here. This is because the AT is calculated by using daily minimum relative humidity instead of relative humidity occurring at the time of the daily maximum temperature, which is not available

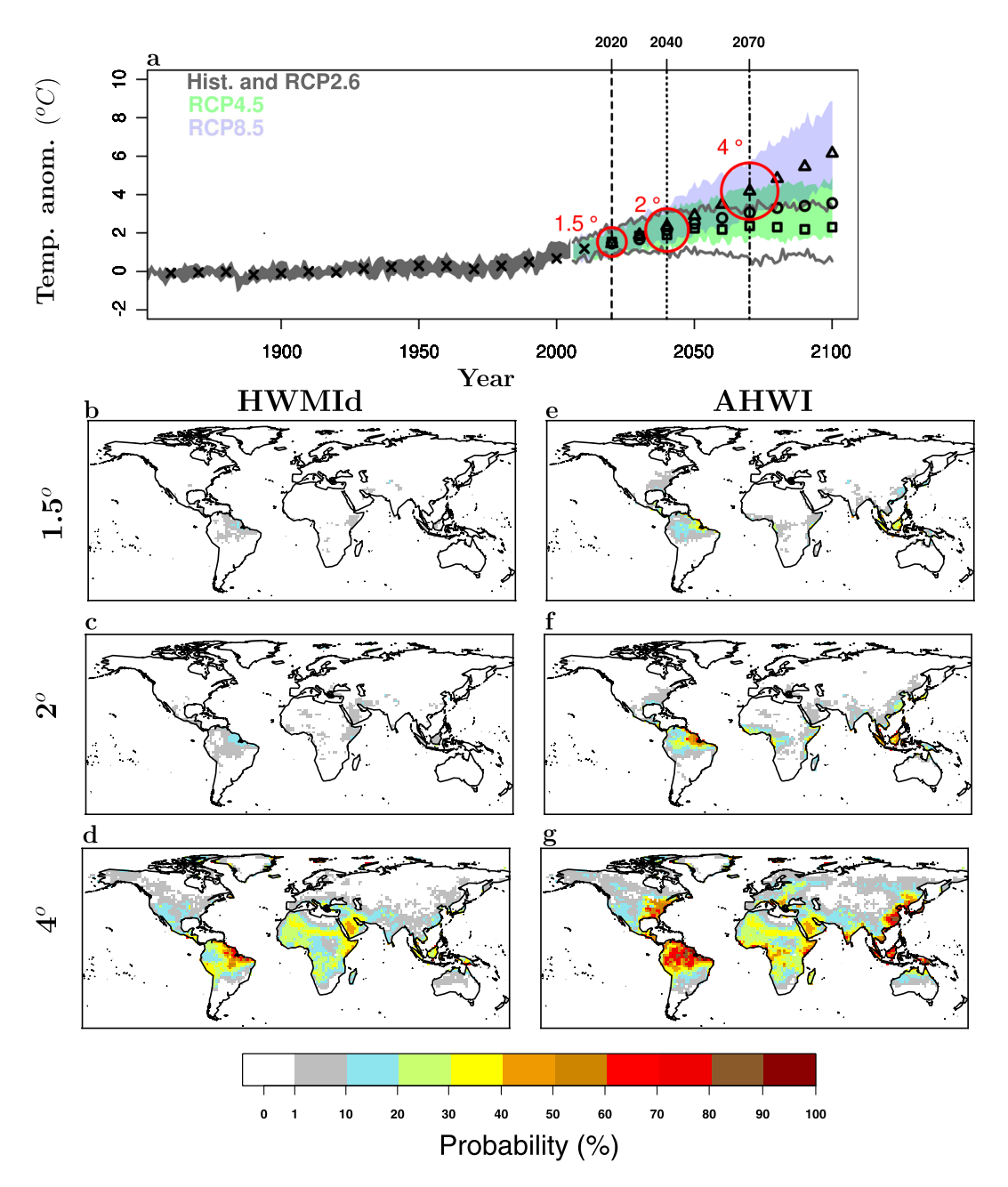


Figure 2. Probability of occurrence of extreme humid heat waves at different warming levels relative to 1861–1880. (a), Simulated global mean surface temperature increase as a function of time. Decadal model median over the historical period (1860–2010) are represented by black crosses. Decadal model median over the future period (2011–2100) for the three Representative Concentration Pathway (RCP2.6, RCP4.5 and RCP8.5) scenarios are represented by black squares, circle and triangles, respectively. (b–d), Probability of occurrence of heat waves with magnitude greater than the maximum magnitude detected in Russia in 2010 (HWMId > 60) calculated at each grid point for all model years with global mean temperature anomaly relative to 1861–1880 between 1.4° and 1.6° (1.5° warming level, see method), 1.9°–2.1° (2° warming level) and 3.9°–4.1° (4° warming level), respectively. e-g, as b-d but for humid heat waves and the relative Apparent Heat Wave Index (AHWI > 60). This figure has been produced using R version 3.3.2 (https://cran.r-project.org/).

in the current models. Further, this study is on heat wave hazards and does not take into account the effects of adaptation or other socio-economic factors^{32, 33}, (for example, improved housing or access to air-conditioning). Our results give an indication of where relative humidity might be an important amplifying factor for heat stress. Changes in heat wave hazard are very important and informative, indicating regions where adaptation measures might be necessary to cope with heat stress.

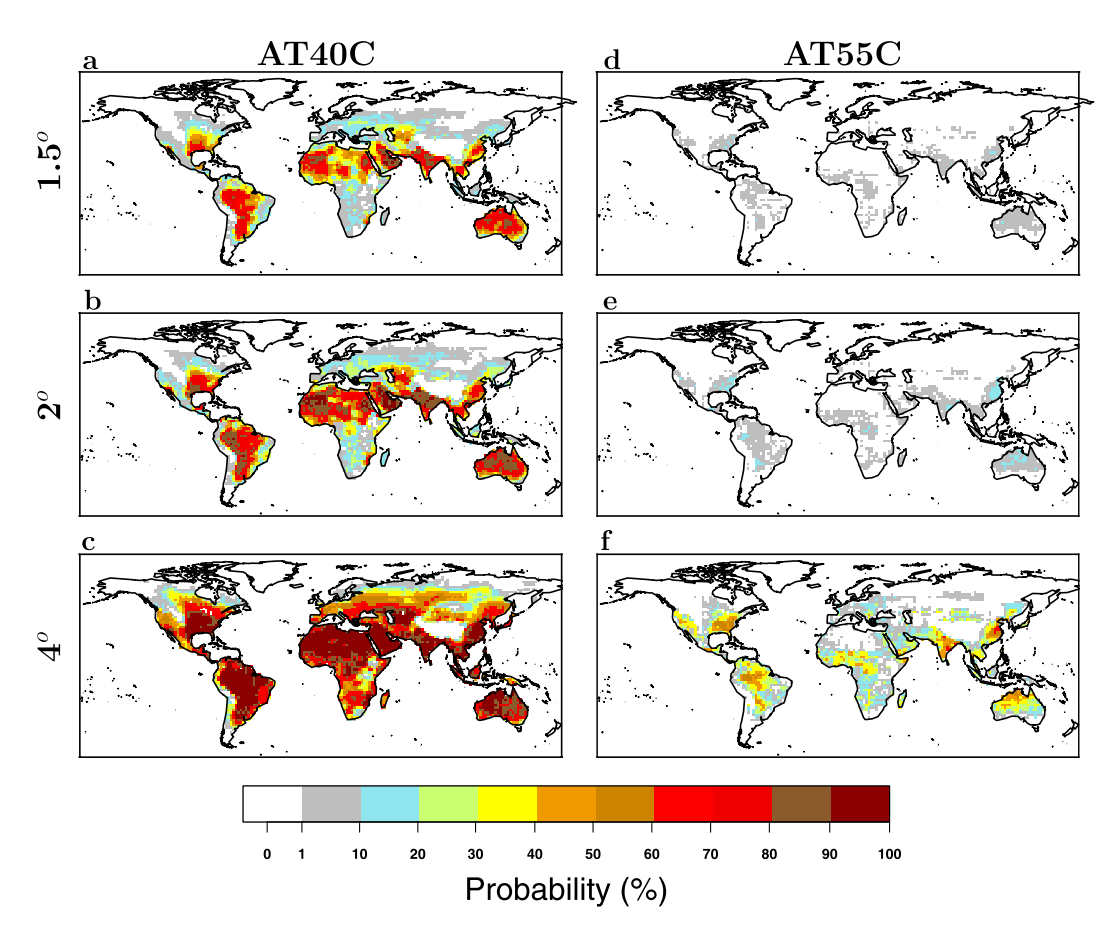


Figure 3. Annual probability of occurrence of a heat waves with apparent temperature peaks greater than $40\,^{\circ}\text{C}$ and $55\,^{\circ}\text{C}$. (a-c), Probability of occurrence of heat waves with $AT_{peak} \geq 40$ (AT40C) calculated at each grid point for all model years with global mean temperature anomaly relative to 1861-1880 at 1.5, 2, and 4 degrees warming (see Fig. 2), respectively. (d-f), as (a-c) but for occurrence of heat waves with $AT_{peak} \geq 55$ (AT55C). This figure has been produced using R version 3.3.2 (https://cran.r-project.org/).

Methods

Daily maximum temperature and minimum relative humidity data from the ERA-Interim (ERA-I) reanalysis from the European Centre for Medium-Range Weather Forecasts 16 , the NCEP-2 reanalysis from the National Centers for Environmental Prediction-Department of Energy, and from nine climate model simulations contributing to CMIP5 (see Supplementary Table 1) are used to study heat waves in the present and future climate. The selection of these nine CMIP5 models is based on the availability of daily maximum temperature and minimum relative humidity data. Reanalysis data have a 6-hourly time resolution and are available from 1979 onward. The ERA-I is based on a T255 resolution (~79 km) grid. For comparison the data are bilinearly interpolated onto the NCEP-2 grid, which has a resolution of 1.875 degrees (~208 km). Similarly, daily maximum temperature and minimum humidity from climate model output were remapped to a common 1.875° × 1.875° analysis grid (T63) to allow comparison with the reanalysis.

We calculate the Heat Wave Magnitude Index daily¹⁵ (HWMId), which depends only on temperature, and the new Apparent Heat Wave Index (AHWI), which is based on temperature and humidity. HWMId was calculated for the historical scenario¹⁸ from 1850 to 2005, and for three Representative Concentration Pathway scenarios¹⁸ (RCP2.6, RCP4.5 and RCP8.5) from 2006 to 2100. The calculation of the AHWI has been done for the same periods and scenarios as for the HWMId, with the exception that for the historical period we started in 1970, since the humidity data were not available for all the used models before this year. We use one run (r1i1p1) for each model. Global mean temperatures (in Fig. 2a) were calculated as the area-weighted global averages of annual mean temperatures.

Heat Wave Magnitude Index daily. The HWMId is defined as the maximum magnitude of heat waves in a year¹⁵, where a heat wave is a period of at least 3 consecutive days with temperature exceeding the daily threshold for the reference period (1981–2010). The threshold is defined as the 90th percentile of daily temperatures, centered on a 31 day window. The magnitude of each heat wave in a year is the sum of the magnitude of the consecutive days composing a heat wave, with daily magnitude calculated as follow:

$$M_d(T_d) = \begin{cases} \frac{T_d - T_{30y25p}}{T_{30y75p} - T_{30y25p}} & \text{if } T_d > T_{30y25p} \\ 0 & \text{if } T_d \le T_{30y25p} \end{cases}$$
(1)

with T_d being the daily maximum temperature on day d of the heatwave, T_{30y25p} and T_{30y75p} are the 25^{th} and 75^{th} percentile values, respectively, of the time series composed of 30-year annual maximum temperatures within the reference period 1981–2010. The HWMId calculation has been done by using the "hwmid" R function³⁴.

Warm Spell Duration Index. The Warm Spell Duration Index, defined by the Expert Team on Climate Change Detection and Indices (ETCCDI) (http://etccdi.pacificclimate.org/list_27_indices.shtml), counts the number of consecutive days of a heat wave (at least 3 consecutive days) with $T_d > 90^{th}$ percentile daily threshold defined above.

Apparent Temperature. The apparent temperature, often referred to as heat index (HI) combines air temperature and relative humidity in order to determine the human-perceived equivalent temperature¹⁰. There are many different versions of apparent temperature. Here we apply the one used by NOAA (see http://www.wpc.ncep.noaa.gov/html/heatindex_equation.shtml):

$$AT = c_1 + c_2 T + c_3 R + c_4 TR + c_5 T^2 + c_6 R^2 + c_7 T^2 R + c_8 TR^2 + c_9 T^2 R^2$$
(2)

where:

AT is the apparent temperature in degrees Fahrenheit °F;

T is temperature (°F);

R is the relative humidity between 0 and 100;

 $c_1 = -42.379; \ c_2 = 2.04901523; \ c_3 = 10.14333127; \ c_4 = -0.22475541; \ c_5 = -6.83783 \times 10^{-3}; \ c_6 = -5.481717 \times 10^{-2}; \ c_7 = 1.22874 \times 10^{-3}; \ c_8 = 8.5282 \times 10^{-4}; \ c_9 = -0.199 \times 10^{-6}.$

The AT values are transformed in Celsius after calculation. Additionally, for all the temperature range where the AT does not work properly we have applied all the adjustments reported in the fact sheet of the NOAA's web page (http://www.wpc.ncep.noaa.gov/html/heatindex.equation.shtml).

Apparent Heat Wave Index. The Apparent Heat Wave Index is defined analogously to the HWMId, but by replacing the T_d temperature in equation (1) by the apparent temperature as given (equation (2)) for days on which AT > T. The AHWI and the previous HWMId are comparable. A AHWI score twice as large as the one of the HWMId means that the heat wave magnitude is amplified twice by humidity. Ideally the AT and the AHWI should be calculated form the daily maximum temperature and simultaneous relative humidity. As the latter is not available for the CMIP5 models we use the daily minimum relative humidity, as done in other studies¹¹, which at first approximation coincides with the maximum temperature at the diurnal cycle. Note that, in order to remove the bias, consisting in a discontinuity between estimation of the two indicators within the reference period (1981–2010) and the ones out-of-base periods^{35, 36}, the HWI and HWMId in the base period have been calculated by means of a bootstrap re-sampling procedure³⁵.

Apparent Temperature peak. The apparent temperature peak (AT $_{peak}$) is defined as the maximum AT value during a heat wave. For each specific year we calculate the maximum apparent temperature value. From the AT $_{peak}$ we define two binary variables: AT40C and AT55C. For each year the AT40C and AT55C are equal to one if the AT $_{peak}$ > 40 °C and AT $_{peak}$ > 55 °C, respectively. Otherwise they are zero.

Estimation of empirical probability. The yearly probability of occurrence of a heat wave with a peak greater than a certain temperature (40 °C and 55 °C) and a magnitude greater than 60 (recorded only in Russia in 2010) has been estimated for the recent past-period (1979–2015) and at different warming levels (1.5 °C, 2 °C, and 4 °C) by using empirical probability. The empirical probability or empirical frequency³⁷ of an event is defined as the ratio between the number of outcomes in which a specified event occurs (e.g. number of years of the recent past-period with $AT_{peak} > 40$ °C) and the total number of trials (e.g. total number of years of the recent past period (1979–2015)). The sample size of the set composed by model years with global mean temperature at 1.5 °C, 2 °C, and 4 °C warming has been estimated equal to 115, 115 and 116, respectively.

References

Research 111, 1-22 (2006)

- 1. Knowlton, K., Rotkin-Ellman, M. & King, G. The 2006 california heat wave: impacts on hospitalizations and emergency department visits. *Environmental Health Perspectives* 117, 61–67 (2009).
- 2. Leonard, M. et al. A compound event framework for understanding extreme impacts. WIREs Clim. Change 5, 113-128 (2014).
- 3. Conti, S. et al. Epidemiologic study of mortality during the summer 2003 heatwave in italy. Environmental Research. 98, 390–399 (2005).
- 4. Dematte, J. et al. Near-fatal heat stroke during the 1995 heat wave in chicago. Ann. Intern. Med. 129, 173–181 (1998).
- 5. Fischer, E. & Knutti, R. Robust projections of combined humidity and temperature extremes. *Nature Climate Change* **3**, 126–130 (2013).
 6. Frich, P. *et al.* Observed coherent changes in climatic extremes during the second half of the twentieth century. *Climate Research* **19**,
- 193–212 (2002).
 7. Alexander, L. *et al.* Global observed changes in daily climate extremes of temperature and precipitation. *Journal of Geophysical*
- 8. Perkins, S. & Alexander, L. On the measurement of heat waves. Journal of Climate 26, 4500-4517 (2012).
- S. Sillman, J., Kharin, V., Zhang, X., Zwiers, F. & Bronaugh, D. Climate extremes indices in the cmip5 multimodel ensemble: Part 1. model evaluation in the present climate. *Journal of Geophysical Research* 118, 1716–1733 (2013).
- Steadman, R. The assessment of sultriness. part i: A temperature-humidity index based on human physicology and clothing science. J. Appl. Meteorol. 18, 861–873 (1979).
- 11. Fischer, E. & Schär, C. Consistent geographical patterns of changes in high-impact european heatwaves. *Nature Geoscience* 3, 398-403 (2010).
- Barnett, A., Tong, S. & Clements, A. What measure of temperature is the best predictor for mortality? *Environmental Research* 119, 604–611 (2010).
- 13. Davis, R., McGregor, G. & Enfield, K. Humidity: a review and primer on atmospheric moisture and human health. *Environmental Research* 144, 106–116 (2016).

- 14. Pal, J. & Eltahir, E. Future temperature in southwest asia projected to exceed a threshold for human adaptability. *Nature Climate Change* 3, 197–200 (2016).
- 15. Russo, S., Sillmann, J. & Fischer, E. Top ten european heat-waves since 1950 and their occurrence in the coming decades. *Environmental Research Letters* 10, 1–16 (2015).
- 16. Dee, D. P. et al. The era-interim reanalysis: Configuration and performance of the data assimilation system. Q. J. R. Meteorol. Soc. 137, 553–597 (2011).
- 17. Kanamitsu, M. et al. Ncep-doe amip-ii reanalysis (r-2). Bulletin of the American Meteorological Society 83, 1631-1643 (2002).
- 18. Taylor, K., Stouffer, R. & Meehl, G. An overview of cmip5 and the experiment design. *Bulletin of the American Meteorological Society* 93, 495–498 (2012).
- 19. Fischer, E. & Knutti, R. Robust projections of combined humidity and temperature extremes. Nature Climate Change 3, 126-130 (2012).
- 20. Miralles, D., Teuling, A., van Heerwaarden, C. & de Arellano, J. Mega-heatwave temperatures due to combined soil desiccation and atmospheric heat accumulation. *Nature Geoscience* 7, 345–349 (2014).
- 21. Barriopedro, D., Fischer, E., Luterbacher, J., Trigo, R. & García-Herrera, R. The hot summer of 2010: Redrawing the temperature record map of europe. *Science* 332, 220–224 (2011).
- 22. Freychet, S., Tett, S. & Wang, J. G. H. Summer heat waves over eastern china: dynamical processes and trend attribution. *Environmental Research Letters* 12, 1–9 (2017).
- 23. Katsafados, P., Papadopoulos, A., Varlas, G., Papadopoulou, E. & Mavromatidis, E. Seasonal predictability of the 2010 russian heat wave. *Natural Hazard and Earth System Sciences* 14, 1531–1542 (2014).
- 24. Klinenberg, E. Heat wave: A social autopsy of disaster in chicago. University of Chicago Press (2015).
- 25. Sarofim, M. et al. Ch. 2: Temperature-related death and illness. the impacts of climate change on human health in the united states: A scientific assessment. U.S. Global Change Research Program, Washington, DC 21, 43–68 (2016).
- 26. Kaiser, R. et al. The effect of the 1995 heat wave in chicago on all-cause and cause-specific mortality. American Journal of Public Health 97 (Suppl 1), S158–S162 (2007).
- 27. Huang, W., Haidong, K. & Kovats, S. The impact of the 2003 heat wave on mortality in shanghai, china. Science of the Total Environment 408, 2418-2420 (2010).
- 28. Sherwood, S. C. et al. Relative humidity changes in a warmer climate. J. Geophys. Res. 115, 1-11 (2010).
- 29. Delworth, T., Mahlman, J. & Knutson, T. Changes in heat index associated with co2-induced global warming. climatic change. *Climatic Change* 43, 369–386 (1999).
- 30. WHO. Quantitative risk assessment of the effects of climate change on selected causes of death, 2030s and 2050s. World Health Organization, Geneva (2014).
- 31. Sherwood, S. & Huber, M. An adaptability limit to climate change due to heat stress. *Proceedings of the National Academy of Sciences of the United States of America* **107**, 9552–9555 (2010).
- 32. Sheridan, S., Kalkstein, A. & Kalkstein, L. Trends in heat-related mortality in the united states, 1975–2004. *Natural Hazards* **50**, 145–160 (2009).
- 33. Gosling, S. N. C., Lowe, J. A. C., McGregor, G. R. C., Pelling, M. C. & Malamud, B. D. Associations between elevated atmospheric temperature and human mortality: a critical review of the literature. *Climatic Change* **92**, 299–341 (2009).
- 34. Gilleland, E. & Katz, R. W. extremes 2.0: An extreme value analysis package in r. Journal of Statistical Software 72, 1-39 (2016).
- 35. Zhang, X. C., Hegerl, G. C., Zwiers, F. W. C. & Kenyon, J. Avoiding inhomogeneity in percentile-based indices of temperature extremes. *Journal of Climate* 18, 1641–1651 (2005).
- 36. Sippel, S. C. *et al.* Quantifying changes in climate variability and extremes: Pitfalls and their overcoming. *Geophysical Research Letters* **42**, 9990–9998 (2015).
- 37. Mood, A. M. C., Graybill, F. A. C. & Boes, D. Introduction to the theory of statistics (3rd ed.). McGraw-Hill (1974).

Acknowledgements

We acknowledge the World Climate Research Program's Working Group on Coupled Modeling, which is responsible for CMIP5 model outputs. J.S. is supported by the Research Council of Norway grant 243953/E10 (ClimateXL) and grant 244551/E10 (CiXPAG). Thank you to all the colleagues from the Competence Centre on Composite Indicators and Scoreboards (COIN) for their comments during internal presentations. Thanks to Virmantas Kvedaras for his important suggestions during coffee break.

Author Contributions

All authors contributed to the idea and scope of the paper. S.R. performed the analyses. All authors discussed the results and contributed to writing and reviewing the manuscript.

Additional Information

Supplementary information accompanies this paper at doi:10.1038/s41598-017-07536-7

Competing Interests: The authors declare that they have no competing interests.

Publisher's note: Springer Nature remains neutral with regard to jurisdictional claims in published maps and institutional affiliations.

Open Access This article is licensed under a Creative Commons Attribution 4.0 International License, which permits use, sharing, adaptation, distribution and reproduction in any medium or format, as long as you give appropriate credit to the original author(s) and the source, provide a link to the Creative Commons license, and indicate if changes were made. The images or other third party material in this article are included in the article's Creative Commons license, unless indicated otherwise in a credit line to the material. If material is not included in the article's Creative Commons license and your intended use is not permitted by statutory regulation or exceeds the permitted use, you will need to obtain permission directly from the copyright holder. To view a copy of this license, visit https://creativecommons.org/licenses/by/4.0/.

© The Author(s) 2017